ФІЗИКА МАТЕРІАЛІВ

УДК 393.7 PACS 81.20.Ka, 83.10.Tv, 81.07.-b, 81.40.-z

V. Bezpalchuk, A. Gusak, R. Kozubski

CORRELATIONS BETWEEN PHASE FORMATION MORPHOLOGY AND SEQUENCE WITH THE TEMPERATURE PROFILE OF EXOTHERMIC SOLID-STATE REACTIONS

Nowadays it is possible to measure the temperature profile in the front of SHS reaction which is related to the time-dependent temperature rise in exothermic adiabatic reaction. It is shown that in the scaled temperature/time variables, this profile can tell much about the sequence of the phase formation and morphology of reaction zone during the reaction.

Keywords: SHS, multilayer thin films, modeling, diffusion, phase formation, Ni-Al system.

Introduction

Self-sustained High-temperature Synthesis (SHS) in powder mixtures and in lamellar multi-foils is now widely used in various applications, including local melting (by SHS reactions) of solder joints in the microelectronic devices [1-3]. Despite wide applications, the phase formation sequence, as well as detailed reaction mechanisms in SHS or in homogeneous exothermic reactions in nano-foils (simultaneously along all contact surface) remains a subject of intensive discussions [4]. Experimentally, this issue is difficult to solve since the mentioned reactions proceed fast, during the very short period. In this paper, we suggest a way distinguish various exothermic reaction mechanisms and phase formation sequences by analyzing the temperature time dependence in the reaction zone in adiabatic conditions. So far we limit ourselves with so-called homogeneous exothermic reactions proceeding simultaneously along all length of the contact between materials. We represent the time dependence of temperature in the scaled variables.

$$0 \le tt = t / t^{reaction} \le 1,\ 0 \le TT = \frac{T - T_0}{T^{\max} - T_0} \le 1$$

Here $t^{reaction}$ is a time to complete the reaction, $T^{\max}$ is a maximal temperature just after completion of the reaction. We neglect the heat out-flux, so that all heat released during the reaction, remains in the system raising its temperature

1. Adiabatic single phase growth in a planar geometry

Here we consider multilayer or bilayer with a stoichiometric quantity of reactants so that end of reaction A + B → AB means simultaneous full consumption of the initial materials A (for example, Al) and B (for example, Ni) – Fig.1.

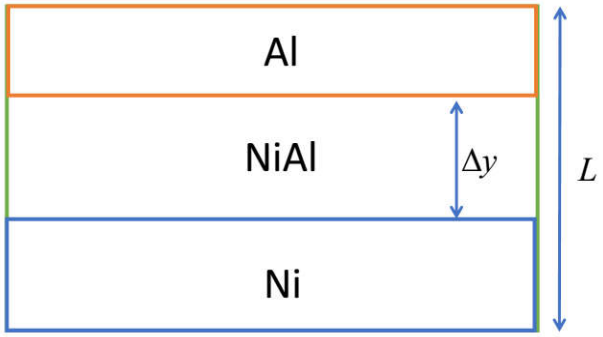

Figure 1. Direct formation of NiAl-phase.

For the sake of simplicity, we will assume the constant and equal atomic volumes of both components. We also will take a Dulong-Petit law for heat capacity taking the heat capacity per atom of all phases as the same and equal $cap = 3k_B$. We also use the phase formation enthalpy per atom, h_1 under adiabatic conditions.

$$T = T_0 + \frac{h_1}{cap}\frac{\Delta y}{L} \tag{1}$$

On the other hand, the kinetics of the diffusion-controlled phase growth is governed by the well-known equation [5].

$$2\Delta y \left| \frac{d\Delta y}{dt} = \frac{D_{w0}\exp\left(-\frac{Q}{kT(t)}\right)}{C(1-C)} \cdot \frac{1}{\Delta y} \right. \tag{2}$$

Equations (1, 2) immediately give eq. (3):

$$\frac{d(\Delta y)^2}{dt} = \frac{2D_{w0}}{C(1-C)}\exp\left(-\frac{Q}{k}\cdot\frac{1}{T_0 + \frac{h_1}{cap}\cdot\frac{\Delta y}{L}}\right) \tag{3}$$

Calculations were made for parameters: Q = 2 eV, h1 = 0.605 eV and ratio Q/h1 = 3.3035.

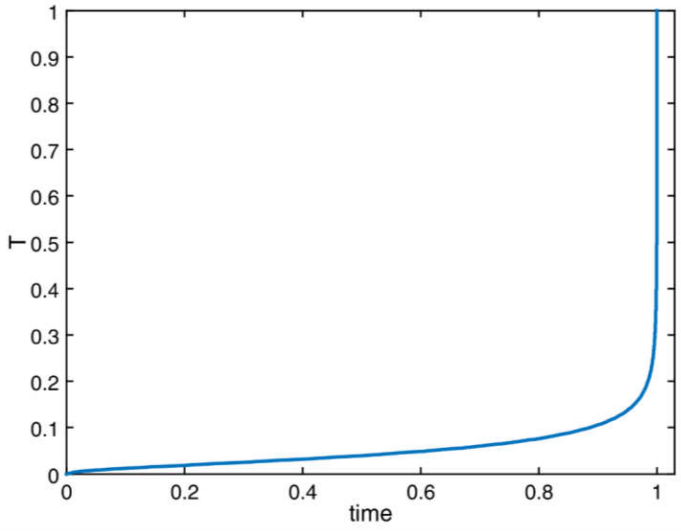

Figure 2. Scaled temperature/time dependence for single solid phase growth under the layer geometry.

2. Adiabatic two phases sequential (one–by-one) growth in a planar geometry

Now consider the formation of the final NiAl phase in two-stage reaction: At the first stage a single phase NiAl3 grows via solid-state reaction Ni + 3Al → NiAl3, suppressing the phase NiAl till the full consumption of pure Al. After this the phase NiAl3 becomes marginal and now is consumed for the formation of NiAl phase via reaction 2Ni + NiAl3 → 3NiAl.

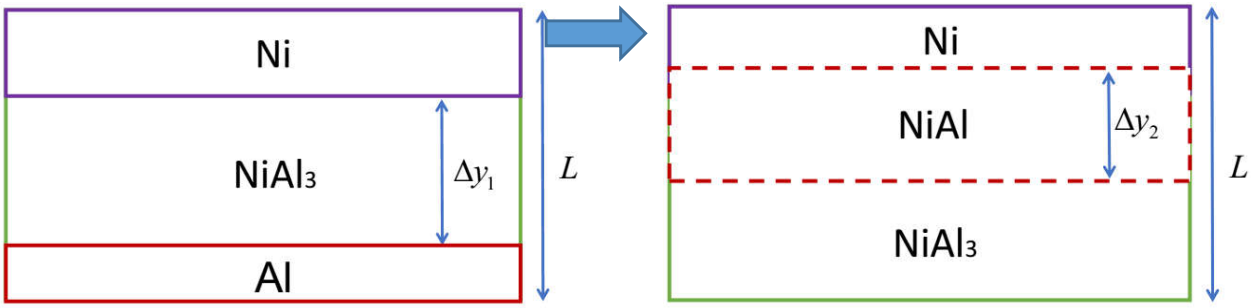

Figure 3. Sequential (one-by-one) formation of the phase $NiAl_3$ and NiAl.

I stage – formation of the phase $NiAl_3$ via solid-state reaction Ni+3Al → $NiAl_3$: ($\Delta y_1 \le \frac{2}{3}L$). At this stage, the temperature raises proportionally to the thickness of the first growing phase and to the first formation enthalpy.

$$T = T_0 + \frac{h_1'}{cap}\frac{\Delta y_1}{L}, \quad \Delta y_1^{\max} = \frac{2}{3}L \tag{4}$$

$$\frac{d\Delta y_1}{dt} = \frac{D_{1w0}\exp\left(-\frac{Q_1}{kT(t)}\right)}{C_1(1-C_1)}\cdot\frac{1}{\Delta y_1} \tag{5}$$

II stage – formation of the phase NiAl via reaction 2Ni + NiAl3 → 3NiAl:

$$T = T_0 + \frac{h_1'}{cap}\frac{\frac{2}{3}L}{L} + \frac{h_2'}{cap}\frac{\Delta y_2}{L} \tag{6}$$

$$\frac{d\Delta y_2}{dt} = \frac{(1-C_1)}{(1-C_2)(C_2-C_1)}\frac{D_{2w0}\exp\left(-\frac{Q_2}{kT(t)}\right)}{\Delta y_2} \tag{7}$$

We made calculations for the realistic case of low melting first phase with a lower activation energy, higher preexponential factor:

$$D_{1w0} > D_{2w0}, \quad Q_1 < Q_2, \quad h_2' > \frac{1}{3}h_1'$$

where $Q_1 = 2$eV, $Q_2 = 4$eV, D_{1w0}=1e-4, D_{2w0}=0.3e-4, $h_1' = 0.543$ eV, $h_2' = 0.2434$ eV (Fig. 4).

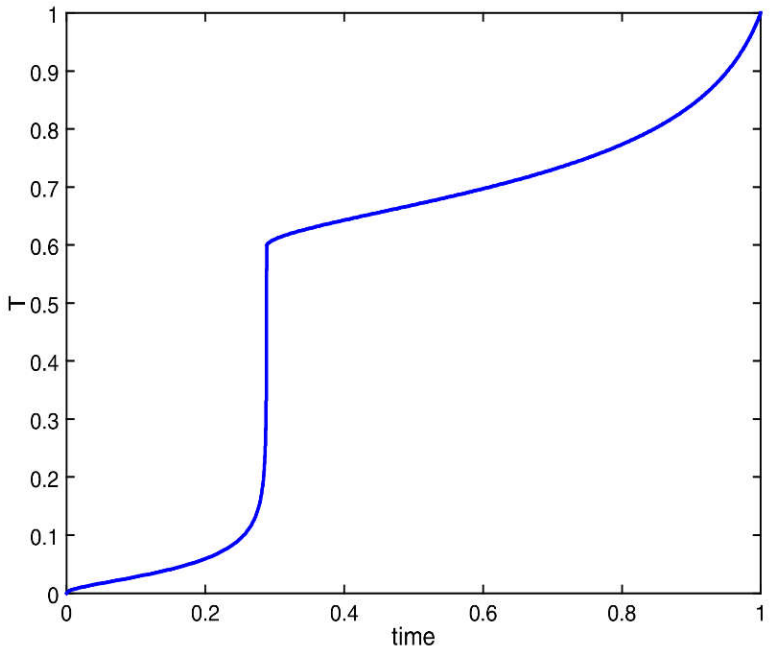

Figure 4. Scaled temperature versus scaled time dependence for two-staged (one-by-one) reaction.

3. Formation of single final phase in the reaction Ni+ liquid Al-based solution with formation and growth of NiAl scallops with liquid channel between them

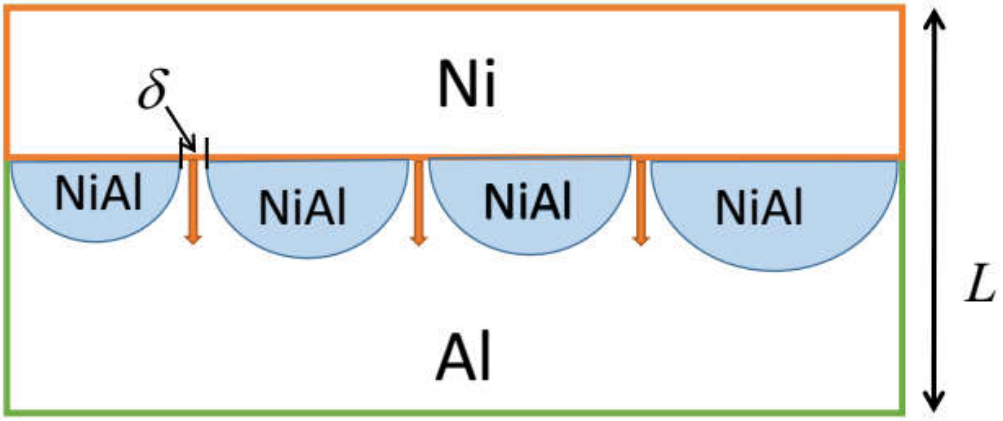

Figure 5. The growth of NiAl scallops with a liquid channel between them.

The idea of the mathematical model can be found as analogical to the growth of Cu6Sn5 scallops in reaction 6Cu + 5Sn → Cu6Sn5 [6]. In the crudest approximation of equi-sized scallops, one obtains: Number of scallops per area S and total volume of the growing phase are

$$M \approx \frac{S}{\pi R^2}, \quad V^{new} \approx M \frac{2}{3}\pi R^3 = \frac{2}{3} SR \tag{8}$$

The flux of Ni into liquid via the channels is

$$I_{Ni} \approx 2M\pi R \frac{\delta}{2} \cdot \frac{1}{\Omega} D_{Ni}^{melt} \left(C_{Ni}^{Ni/Al^m} - C_{Ni}^{NiAl/Al^m} \right) \cdot \frac{1}{R} \tag{9}$$

This flux is related to the increment of the new phase volume and number of atoms in this new phase:

$$I_{Ni}dt = \frac{C}{\Omega}dV^{new}$$
$$dN^{new} = \frac{dV^{new}}{\Omega} \quad (10)$$

The increment of new phase volume and of a number of atoms is proportional to the increment of temperature:

$$N^{total} cap \cdot dT = dQ = h_1 dN = h_1 \frac{dV^{new}}{\Omega} = h_1 \frac{I_{Ni}}{C} dt \quad (11)$$

so that

$$\frac{SL}{\Omega} cap \cdot dT = \frac{h_1 S}{C\pi R^2} 2\pi R \frac{\delta}{2} \frac{1}{\Omega} \frac{D_{Ni}^{melt} \Delta C}{R} dt \quad (12)$$

.

Thus, the final equations allow to calculate the reaction kinetics just analytically:

$$dT = \frac{1}{L} \frac{h_1}{cap \cdot C} \frac{\delta D_{Ni}^{melt} \Delta C}{R^2} dt, \quad D_{Ni}^{melt} - const \quad (13)$$

$$\frac{C}{\Omega} \frac{2}{3} S \frac{dR}{dt} = \frac{S}{\pi R^2} 2\pi R \frac{\delta}{2\Omega} \frac{D_{Ni}^{melt} \Delta C}{R} \quad (14)$$

$$3R^2 \left| dR = \frac{3}{2} \frac{\delta D_{Ni}^{melt} \Delta C}{R^2} dt, \quad dR^3 = \frac{9}{2} \delta D_{Ni}^{melt} \Delta C dt \right. \quad (15)$$

$$R(0) = 0, \qquad R = \left(\frac{9}{2} \delta D_{Ni}^{melt} \Delta C t \right)^{1/3} \quad (16)$$

$$dT = \frac{1}{L} \frac{h_1}{cap} \frac{1}{C} \frac{\left(\delta D_{Ni}^{melt} \Delta C \right)}{\left(\frac{9}{2} \delta D_{Ni}^{melt} \Delta C t \right)^{2/3}} dt \quad (17)$$

$$T = T_0 + \frac{h_1}{cap} \frac{3}{CL} \left(\frac{2}{9} \right)^{2/3} \left(\delta D_{Ni}^{melt} \Delta C t \right)^{1/3} \quad (18)$$

Typical curve scaled temperature-scaled time can be seen at the Fig.4. with the following parameters: $h_1 = 0.48$eV, δ = 1e-9, D_{Ni}^{melt} = 4.5e-9.

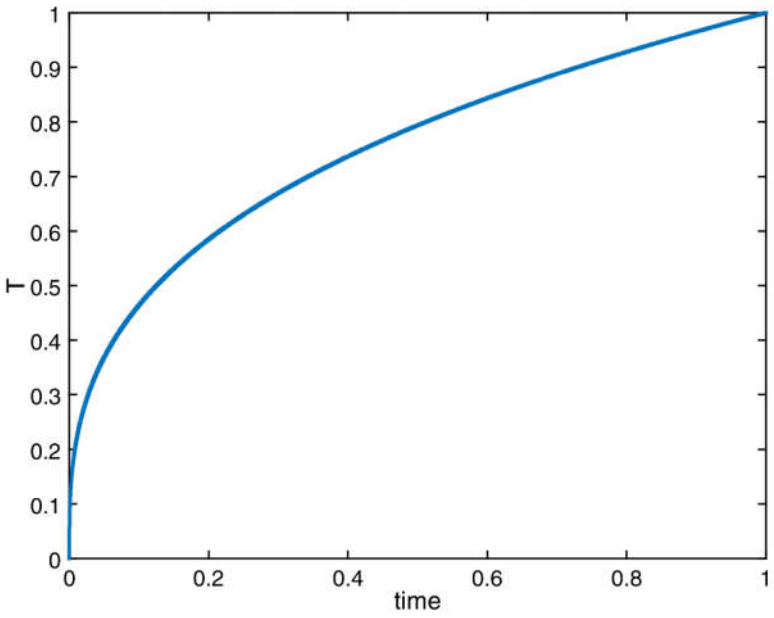

Figure 6. Scaled temperature versus scaled time for the single phase growth in the form of scallops due to diffusion via the liquid channels between scallops.

4. Dissolution of Ni in the molten Al-based solution followed by crystallization of obtained liquid solution

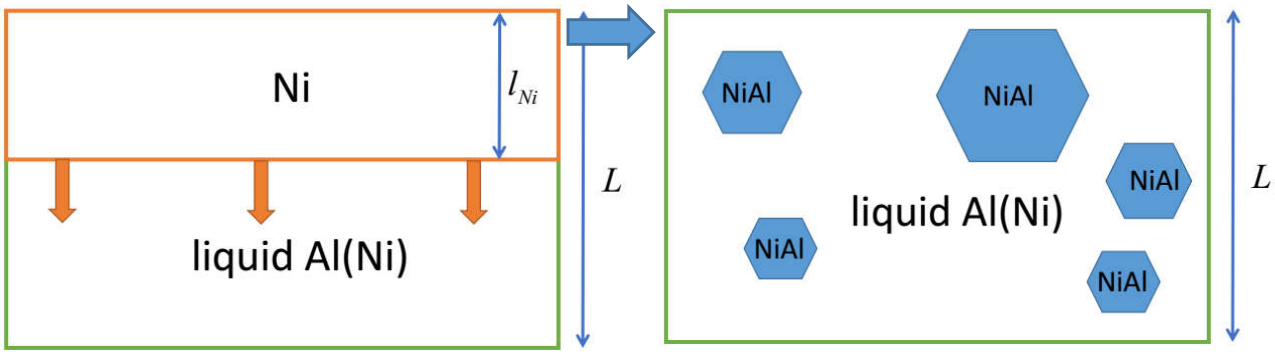

Fig.7. Formation of NiAl compound by (1) dissolution of Ni in liquid Al till the full dissolution of Ni [4], and (2) crystallization of the unstable solution into the ordered phase via Avrami kinetics.

We will treat the dissolution as the interface-controlled process

$$\frac{(-dl_{Ni})}{dt} = k(T) = k_0 \exp\left(-\frac{Q_k}{k_B T}\right) \tag{19}$$

Of course, dissolution of Ni in liquid and respective decrement of Ni thickness lead to the temperature increment:

$$\frac{(-dl_{Ni})}{l_{Ni}} = \frac{cap \cdot dT}{h(C)} \tag{20}$$

Since the dissolution of Ni in the liquid Al is very far from Vegard law, it seems more convenient to switch from the thickness to the number of atoms:

$$\frac{S(-dl_{Ni})}{\Omega} = \left(-dN^{Ni}\right)$$

$$dQ = h(C)(-dN^{Ni}) \tag{21}$$

$$dQ = N^{total} cap \cdot dT$$

$$\frac{SL}{\Omega} cap \cdot dT = h_0(1-2C_{Ni})\frac{S}{\Omega}(-dl_{Ni}) \tag{22}$$

$$dT = \frac{h_0(1-2C_{Ni})}{cap}\frac{(-dl_{Ni})}{L} \tag{23}$$

Thus, temperature at the moment of full Ni dissolution (if crystallization will not start earlier) can be found as

$$T^{cross} = T_0 + \frac{h_0}{cap \cdot L}\int_{l_0^{Ni}}^{0}(1-2C_{Ni})(-dl_{Ni}) \tag{24}$$

Here the concentration of Ni in the solution can be easily expressed in terms of remaining thickness of Ni film.

$$C_{Ni} = \frac{\frac{L}{2}-l_{Ni}}{L-l_{Ni}}, \quad 1-C_{Ni} = \frac{L/2}{L-l_{Ni}} \tag{25}$$

$$T^{cross} - T_0 = \frac{h_0}{cap}\frac{\ln 2}{2} \tag{26}$$

Since the dissolution includes the intermixing of components, the crystallization enthalpy is less than the compound formation enthalpy from pure components:

$$h^{cryst} = h_1 - h_0\frac{\ln 2}{2} \tag{27}$$

Further, we use the classical Kolmogorov - Avrami scheme with a constant velocity of crystal growth V (which is, of course, a rather crude approximation):

$$\frac{V^{new}}{V^{total}} = 1-\exp\left(-\frac{4\pi}{3}\nu V^3 t^4\right) \tag{28}$$

Heat balance gives:

$$N^{total} cap \cdot dT = dQ = h^{cryst}\frac{dV^{new}}{\Omega} \tag{29}$$

Thus,

$$dT = \frac{h^{cryst}}{cap}4\pi\nu V^3 t^3 \exp\left(-\frac{4\pi}{3}\nu V^3 t^3 t\right)dt \tag{30}$$

$$T_{end} = T_0 + \frac{h_1}{cap} \tag{31}$$

$$T^{new} = T + \frac{h^{cryst}}{cap}\left(\frac{4\pi\nu V^3 t^3}{3}\exp\left(-\frac{\pi\nu V^3 t^4}{3}\right)\right)dt \tag{32}$$

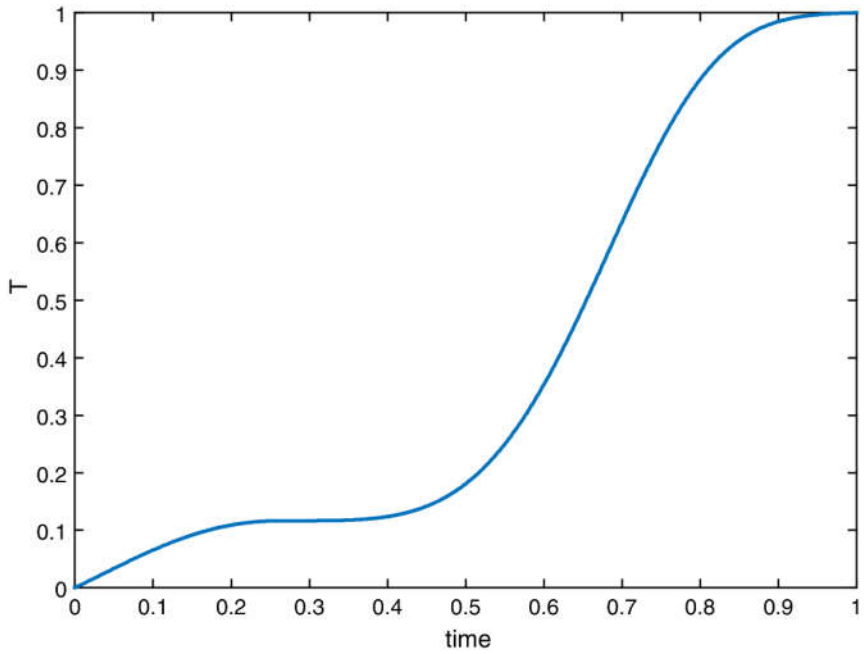

Figure 8. Typical scaled temperature-scaled time in "dissolution plus crystallization" model (h_1 = 0.6055eV, $h_1 = 0.6h_0$, $\pi\nu V^3$ = 1e+29, Q=0.312 eV, k_0=10)

Conclusions

Comparison of figures 2, 4, 6, 8 demonstrate that different phase formation sequence and different morphology of reaction zone correspond to the different time dependence of temperature in the scaled form. Evidently, the same conclusion can be predicted for the exothermic in non-homogenous SHS regime. Thus measuring of the temperature profile in the SHS for can be used for determination of phase formation sequence in the SHS process.

Acknowledgment

This work was supported by the Marie Curie International Research Staff Exchange Scheme Fellowship IRSES within the 7th European Community Framework Programme under Grant 612552; Ministry of Education and Science of Ukraine under Grant 0115U000638 and Grant 0116U004691.

References

1. Tu, K. N., & Gusak, A. M. (2014). *Kinetics in nanoscale materials*. John Wiley & Sons.

2. Weihs, T. P., Knio, O., Reiss, M., & Van Heerden, D. (2006). *U.S. Patent No. 6,991,855*. Washington, DC: U.S. Patent and Trademark Office.

3. Zaporozhets, T. V., Gusak, A. M., & Ustinov, A. I. (2011). Conditions of propagation of the SHS reaction front in nanolayered foils in contact with heat-conducting material. *The Paton Welding J*, *8*, 37-41.

4. Turlo, V., Politano, O., & Baras, F. (2016). Modeling self-sustaining waves of exothermic dissolution in nanometric Ni-Al multilayers. *Acta Materialia*, *120*, 189-204.

5. Gusak, A. M., Zaporozhets, T. V., Lyashenko, Y. O., Kornienko, S. V., Pasichnyy, M. O., & Shirinyan, A. S. (2010). *Diffusion-controlled solid state reactions: in alloys, thin-films, and nanosystems*. John Wiley & Sons.

6. Gusak, A. M., & Tu, K. N. (2002). Kinetic theory of flux-driven ripening. *Physical Review B*, *66*(11), 115403.

7. Michaelsen, C., Barmak, K., & Weihs, T. P. (1997). Investigating the thermodynamics and kinetics of thin film reactions by differential scanning calorimetry. *Journal of Physics D: Applied Physics*, *30*(23), 3167.

References

1. Tu K. N. Kinetics in nanoscale materials / K. N. Tu, A. M. Gusak. – John Wiley & Sons, 2014. – 312 p.

2. U.S. Patent No. 6,991,855. Reactive multilayer foil with conductive and nonconductive final products / T. P. Weihs, O. Knio, M. Reiss, D. Van Heerden; Washington, DC: U.S. Patent and Trademark Office. – № US 10/761,439; 21.01.2004; 31.01.2006

3. Zaporozhets T. V. Conditions of propagation of the SHS reaction front in nanolayered foils in contact with heat-conducting material / T. V. Zaporozhets, A. M. Gusak, A. I. Ustinov // The Paton Welding J. – 2011. – Vol. 8. – P. 37–41.

4. Turlo V. Modeling self-sustaining waves of exothermic dissolution in nanometric Ni-Al multilayers / V. Turlo, O. Politano, F. Baras // Acta Materialia. – 2016. – Vol. 120. – P. 189–204.

5. Gusak A. M. Diffusion-controlled solid state reactions: in alloys, thin-films, and nanosystems / A. M. Gusak, T. V. Zaporozhets, Y. O. Lyashenko, S. V. Kornienko, M. O. Pasichnyy, A. S. Shirinyan. – John Wiley & Sons, 2010. – 498 p.

6. Gusak A. M. Kinetic theory of flux-driven ripening / A. M. Gusak, K. N. Tu // Physical Review B. – 2002. – Vol. 66. – P. 115403.

7. Michaelsen C. Investigating the thermodynamics and kinetics of thin film reactions by differential scanning calorimetry / Michaelsen, C., Barmak, K., & Weihs, T. P. // Journal of Physics D: Applied Physics. – 1997. – Vol. 30. – P. 3167.

Анотація. ***В. М. Безпальчук, А. М. Гусак, Р. Козубский. Кореляції між морфологією і послідовністю фазоутворення та температурним профілем екзотермічних твердотільних реакцій.*** *Самопоширюваний високотемпературний синтез (СВС) в порошкових сумішах і в пластинах мультишарових фольг в даний час широко використовуються в різних технологічних процесах, включаючи точкове плавлення (за допомогою реакції СВС), паяння з'єднань в мікроелектронних пристроях. Незважаючи на широке застосування, послідовність фазоутворення, а також детальні механізми перебігу реакції в СВС або в однорідних екзотермічних реакціях в нанофольгах (одночасно уздовж всієї контактної поверхні) залишається предметом інтенсивних дискусій. В даний час існує можливість вимірювати температурний профіль вздовж фронту реакції СВС, яка пов'язана із часовою залежністю підвищення температури в екзотермічної адіабатичній реакції. В даній роботі показано, що у приведеній, обезрозміреній формі, профіль температура/час може багато що сказати про послідовність формування фаз і морфології реакційної зони в процесі реакції.*

Одержано редакцією 01.08.2016 Прийнято до друку 19.09.2016